Neurobiology of Disease

Sodium Channel $Na_V1.8$ Underlies TTX-Resistant Axonal Action Potential Conduction in Somatosensory C-Fibers of Distal Cutaneous Nerves

Amanda H. Klein,[1]* Alina Vyshnevska,[2]* Timothy V. Hartke,[1] Roberto De Col,[2] Joseph L. Mankowski,[3] Brian Turnquist,[4] Frank Bosmans,[5] Peter W. Reeh,[6] Martin Schmelz,[2] Richard W. Carr,[2] and Matthias Ringkamp[1]

[1]Department of Neurosurgery, Johns Hopkins University, Baltimore, Maryland 21287, [2]Department of Anaesthesiology and Operative Intensive Care, University of Heidelberg, 68167 Mannheim, Germany, [3]Department of Molecular and Comparative Pathobiology and [5]Department of Physiology and Solomon H. Snyder Department of Neuroscience, Johns Hopkins University, Baltimore, Maryland 21205, [4]Department of Mathematics and Computer Science, Bethel University, St. Paul, Minnesota 55112, and [6]Institute of Physiology and Pathology, University of Erlangen-Nuremberg, 91054 Erlangen, Germany

Voltage-gated sodium (Na_V) channels are responsible for the initiation and conduction of action potentials within primary afferents. The nine Na_V channel isoforms recognized in mammals are often functionally divided into tetrodotoxin (TTX)-sensitive (TTX-s) channels ($Na_V1.1$–$Na_V1.4$, $Na_V1.6$–$Na_V1.7$) that are blocked by nanomolar concentrations and TTX-resistant (TTX-r) channels ($Na_V1.8$ and $Na_V1.9$) inhibited by millimolar concentrations, with $Na_V1.5$ having an intermediate toxin sensitivity. For small-diameter primary afferent neurons, it is unclear to what extent different Na_V channel isoforms are distributed along the peripheral and central branches of their bifurcated axons. To determine the relative contribution of TTX-s and TTX-r channels to action potential conduction in different axonal compartments, we investigated the effects of TTX on C-fiber-mediated compound action potentials (C-CAPs) of proximal and distal peripheral nerve segments and dorsal roots from mice and pigtail monkeys (*Macaca nemestrina*). In the dorsal roots and proximal peripheral nerves of mice and nonhuman primates, TTX reduced the C-CAP amplitude to 16% of the baseline. In contrast, >30% of the C-CAP was resistant to TTX in distal peripheral branches of monkeys and WT and $Na_V1.9^{-/-}$ mice. In nerves from $Na_V1.8^{-/-}$ mice, TTX-r C-CAPs could not be detected. These data indicate that $Na_V1.8$ is the primary isoform underlying TTX-r conduction in distal axons of somatosensory C-fibers. Furthermore, there is a differential spatial distribution of $Na_V1.8$ within C-fiber axons, being functionally more prominent in the most distal axons and terminal regions. The enrichment of $Na_V1.8$ in distal axons may provide a useful target in the treatment of pain of peripheral origin.

Key words: nociceptor; nonhuman primate; pain; sodium channels

Significance Statement

It is unclear whether individual sodium channel isoforms exert differential roles in action potential conduction along the axonal membrane of nociceptive, unmyelinated peripheral nerve fibers, but clarifying the role of sodium channel subtypes in different axonal segments may be useful for the development of novel analgesic strategies. Here, we provide evidence from mice and nonhuman primates that a substantial portion of the C-fiber compound action potential in distal peripheral nerves, but not proximal nerves or dorsal roots, is resistant to tetrodotoxin and that, in mice, this effect is mediated solely by voltage-gated sodium channel 1.8 ($Na_V1.8$). The functional prominence of $Na_V1.8$ within the axonal compartment immediately proximal to its termination may affect strategies targeting pain of peripheral origin.

Introduction

Noxious stimuli are transduced at nociceptor terminals and the resulting action potential discharge is transmitted by axons to the dorsal spinal cord. For the detection of tissue-damaging stimuli in the external environment, nerve terminals express select sets of ion channels, receptors, and neuropeptides. The family of voltage-

Received Dec. 12, 2016; revised April 3, 2017; accepted April 4, 2017.

Author contributions: A.H.K., A.V., M.S., R.W.C., and M.R. designed research; A.H.K., A.V., T.V.H., R.W.C., and M.R. performed research; R.D.C., J.L.M., B.T., F.B., and P.W.R. contributed unpublished reagents/analytic tools; A.H.K., A.V., T.V.H., R.W.C., and M.R. analyzed data; A.H.K., A.V., F.B., M.S., R.W.C., and M.R. wrote the paper.

This work was supported by the National Institutes of Health (Grant R01NS097221 to J.L.M., F.B., and M.R.; Grant P40 OD013117 to RJ Adams; and F32 Fellowship Grant F32DA036991 to A.H.K.) and the German Research Society (DFG Grant SFB1158/1-TP 01 to M.S. and Grant SFB1158/1-TP 04 to R.C.). We thank the Blaustein Pain Research and Education Fund, the Brain Science Institute and the Neurosurgery Pain Research Institute at the Johns Hopkins

gated sodium (Na_V) ion channels is responsible for the generation and propagation of action potentials (Ahern et al., 2016). In nociceptors, the predominant Na_V channel currents originate from $Na_V1.7$, which is sensitive to tetrodotoxin (TTX-s), $Na_V1.8$, and $Na_V1.9$, both of which are TTX-resistant (TTX-r). $Na_V1.8$ expression appears to be important for action potential generation in small, unmyelinated C-fiber neurons (Renganathan et al., 2001). The relatively hyperpolarized activation range of $Na_V1.9$ allows it to pass a persistent current, but a role for $Na_V1.9$ in mediating action potential conduction remains a matter of debate (Priest et al., 2005). The $Na_V1.5$ isoform is also relatively resistant to blockade by TTX (IC_{50} ~2 μM). $Na_V1.5$ can deliver a large transient current in neonatal and early postnatal dorsal root ganglion (DRG) neurons, but its expression falls in adult DRG neurons (Renganathan et al., 2002), although a splice variant is reported in adult mouse DRG (Kerr et al., 2007).

Within DRG neurons, the distribution and functional availability of Na_V channel isoforms differs between somal and axonal compartments. Axonally targeted $Na_V1.8$ mRNA (Ruangsri et al., 2011) and protein (Gold et al., 2003) in peripheral nerves can be significantly higher compared to the soma. Functional studies suggest a differential spatial distribution of Na_V channel isoforms in somatosensory neurons. Electrophysiological recordings from isolated DRG neuronal somata implicate TTX-r isoforms as the primary mediators of inward sodium current during an action potential (Scholz et al., 1998; Blair and Bean, 2002). In contrast, assays of axonal conduction by means of TTX indicate that, for the majority of mammalian C-fibers, action potential propagation relies primarily on TTX-s Na_V channel isoforms (Villière and McLachlan, 1996; Farrag et al., 2002; Zimmermann et al., 2007; De Col et al., 2008). Application of TTX to mammalian peripheral nerves (Yoshida and Matsuda, 1979; Steffens et al., 2001) and dorsal roots (Pinto et al., 2008) results either in overt blockade of C-fiber conduction or a profound slowing of the C-fiber response and a decrease in amplitude. Typically, the compound C-fiber amplitude is reduced to 20–30% of its value before TTX, although values of up to 80% (mean 47%) have been reported in samples of human nerve taken at biopsy or after amputation (Quasthoff et al., 1995). The requirement of TTX-s Na_V channels for axonal conduction in the majority of C-fiber axons manifests functionally in the spinal dorsal horn, where the likelihood of transmitter release in response to C-fiber stimulation is either reduced (Jeftinija, 1994) or largely abolished (Pinto et al., 2008) by TTX. Although $Na_V1.8$ is postulated to serve a role in sensory nerve terminals by remaining available for activation despite cooling, the role of TTX-r Na_V channel isoforms in axonal C-fiber conduction is less clear.

We studied C-fiber-mediated compound action potentials (C-CAPs) along different segments of axonal membrane (distal peripheral nerve, proximal peripheral nerve, and dorsal root) in samples from mice and compared the results to those obtained from nonhuman primates. We discovered that a substantially greater portion of the C-CAP was resistant to TTX in distal compared with proximal nerves. Studies in $Na_V1.9$ and $Na_V1.8$ knock-out mice showed that the TTX-r component of the C-CAP is mediated solely by $Na_V1.8$. These findings demonstrate that the TTX-resistant $Na_V1.8$ isoform not only plays a role in action potential generation in peripheral terminals, but can also support action potential conduction in distal peripheral unmyelinated axons.

Materials and Methods

Study approval. The Animal Care and Use Committee of Johns Hopkins University (JHU) approved the experiments on nervous tissue from mice (C57BL6, $Na_V1.9^{-/-}$) and nonhuman primates. The Ethics Committee of the Regional Government (Karlsruhe, Baden-Wuerttemberg, Germany) approved experiments involving C57BL6 and $Na_V1.8^{-/-}$ mice performed at the University Heidelberg Medical Faculty Mannheim.

Mouse nerve dissection. Adult inbred C57BL6 mice of both sexes and weighing 25–35 g were obtained from Harlan and Janvier. $Na_V1.8^{-/-}$ mice (Akopian et al., 1999) were bred at the University of Erlangen–Nuremberg (Germany) and animals of both sexes weighing 25–35 g (~5–6 weeks) were used. As part of an ongoing research project, $Na_V1.9^{-/-}$ mice were generated by inserting a Neo-STOP minigene upstream of *SCN11A*, thereby reducing expression by ~80%. Mice were anesthetized with isoflurane (5%; Midwest Veterinary Supply) and killed by cervical dislocation. Dorsal roots together with proximal (i.e., sural, saphenous, peroneal, and tibial; Fig. 1*A*) nerve segments and distal peripheral nerve segments (Fig. 1*B*) were dissected from the hind limbs of mice and used within ~24 h (JHU) or 0–2 h (Mannheim) of harvesting. The proximal nerve segments were dissected free over a 15–25 mm length immediately distal to their point of division at the trifurcation of the sciatic nerve at the knee (Fig. 1*A*). Distal nerve segments were harvested from the corium side of a skin flap of the dorsal hindpaw over a length of ~10–15 mm immediately proximal to the tips of the toes so that only one branch innervating the toe was used for recording (Fig. 1*B*).

Primate nerve dissection. Dorsal root and peripheral nerve materials were acquired postmortem from male and female adult pigtail monkeys (*Macaca nemestrina*) that were bred at JHU and had been part of a control cohort in an ongoing SIV research project. Proximal peripheral (i.e., median and ulnar nerves), distal peripheral nerves (i.e., digital nerves), and dorsal roots were dissected and used within ~48 h after harvesting. Tissues not used immediately were stored in synthetic interstitial fluid (see below for details) at room temperature, which was changed after 24 h.

Compound action potential recordings. Isolated nerve segments were maintained in a synthetic interstitial fluid composed of either of the following (in mM): 118 NaCl, 3.2 KCl, 1.5 $CaCl_2$, 1 $MgCl_2$, 6 HEPES, 20 Na^+ gluconate, and 5.6 D-glucose, pH 7.4 (bubbled with 100% O_2) or 107.7 NaCl, 3.5 KCl, 0.69 $MgSO_4$, 26.2 $NaCO_3$, 1.67 NaH_2PO_4, 1.5 $CaCl_2$, 9.64 Na^+ gluconate, 5.5 D-glucose, and 7.6 sucrose, pH 7.4 (bubbled with 95% O_2, 5% CO_2) and subsequently desheathed. C-CAPs were recorded as described previously (Lang et al., 2008; Freysoldt et al., 2009; Carr et al., 2010; Sittl et al., 2012). Briefly, each end of the desheathed nerve segment was drawn into a glass pipette in an organ bath and embedded in petroleum jelly to establish high resistance electrical seals (Fig. 1*C*). Pairs of silver wire electrodes were placed inside each pipette and in the bath. One pair of electrodes was used for constant current stimulation. The other electrode pair recorded extracellular signals (Fig. 1*D*). The distance between the sites of stimulation and recording varied between 3 and 8 mm. The organ bath (~1 ml) was perfused continuously with physiological solution at a flow rate of 2 ml/min. For experiments performed in Mannheim, the temperature of the perfusion solution was controlled with an inline Peltier device. All experiments at JHU were conducted at room temperature. Constant current electrical stimulation (Linear Stimulus Isolator, A395; WPI) was delivered to the nerve with the silver wire inside the stimulating pipette, serving as the anode. Current pulses were applied at either 0.3 or 1 Hz. Extracellular signals were amplified (NeuroLog NL905; Digitimer), filtered (low-pass 5 kHz; high-pass, 0.1 Hz),

University for their support of this study; the National Center for Research Resources and the National Center for Advancing Translational Sciences (NCATS) of the National Institutes of Health (Grant 1UL1TR001079) for statistical analysis; and R.A. Meyer for critically reading a previous version of this manuscript.

The authors declare no competing financial interests.

A.H. Klein's present address: Department of Pharmacy Practice and Pharmaceutical Sciences, University of Minnesota, Duluth, MN 55812.

*A.H.K. and A.V. contributed equally to this work.

Correspondence should be addressed to either of the following: Richard Carr, Department of Anesthesiology, Medical Faculty Mannheim, University of Heidelberg, Ludolf-Krehl Str. 13-17, 68167 Mannheim, Germany. E-mail: Richard.Carr@medma.uni-heidelberg.de; or Matthias Ringkamp, Department of Neurosurgery, School of Medicine, Johns Hopkins University, Meyer 5-109, 600 N Wolfe St, Baltimore, MD 21287. E-mail: platelet@jhmi.edu.

DOI:10.1523/JNEUROSCI.3799-16.2017

 0270-6474/17/375205-11$15.00/0

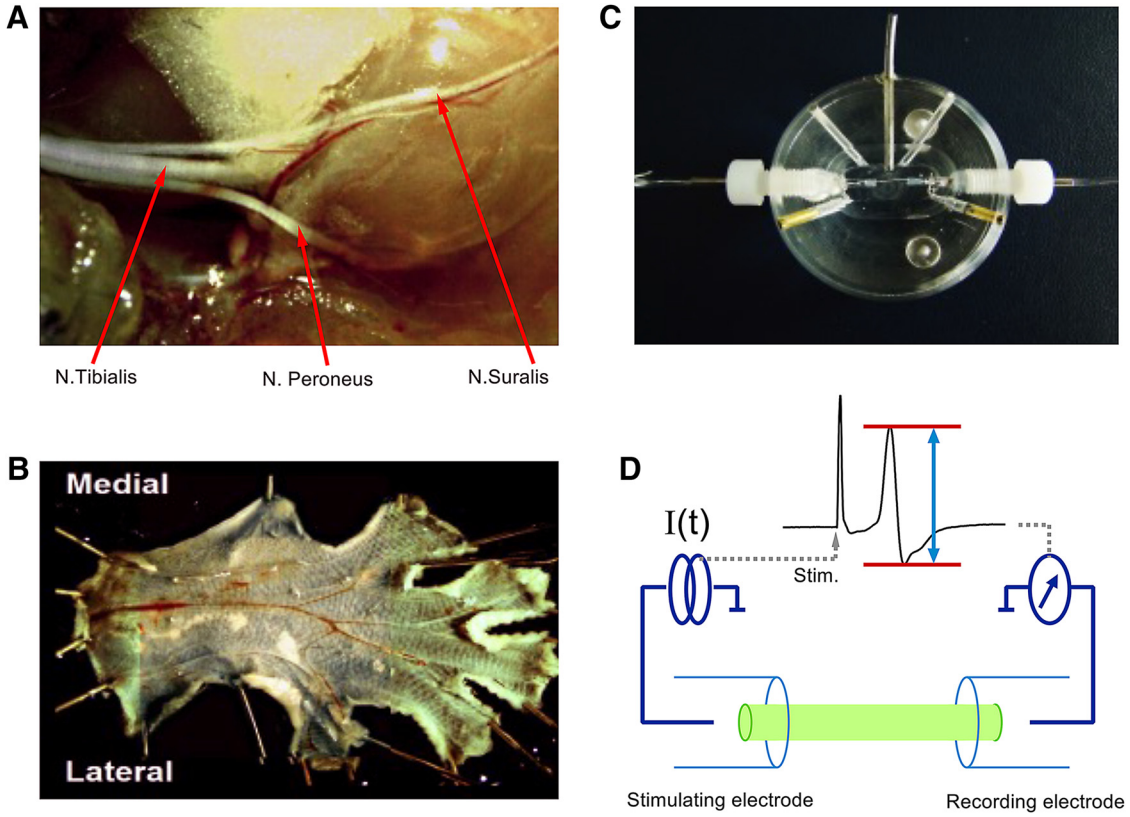

Figure 1. Identification, isolation, and recording arrangement for the peripheral nerve segments in mouse. ***A***, ***B***, Photograph identifying the sural division of the sciatic nerve (***A***) and the distal reaches of nerves innervating the skin of the dorsal hindpaw (***B***). ***C***, Organ bath to register compound extracellular signals. Isolated nerve segments were embedded in petroleum jelly at each end in glass stimulating and recording electrodes. ***D***, Schematic arrangement of recording setup used to deliver electrical stimuli (left) and record ensuing CAP signal (right and inset). Peak-to-peak amplitude of the CAP signal (inset, blue double arrow) was determined within a variable time window (inset, red horizontal bars).

digitized, and stored to disk. Stimulus intensity and data acquisition were controlled using either QTRAC software (Digitimer) or DAPSYS version 8.0 (http://www.dapsys.net).

Experimental protocol. Constant current pulses of fixed amplitude were used to assess conduction in A-fibers (0.1 ms) and C-fibers (1 ms). Under control conditions, CAP responses were recorded until stable amplitude and latency values were established (~5–20 min) at 23 ± 2°C. For JHU experiments using nerves from nonhuman primates and WT and $Na_V1.9^{-/-}$ mice, TTX (1 μM) was applied for at least 5 min or until CAP amplitude had stabilized. This was followed by coapplication of TTX and A803467 (5 μM), a selective $Na_V1.8$ blocker (Jarvis et al., 2007), for at least 5 min or until CAP amplitude had stabilized. TTX and A803467 were subsequently washed out until the C-CAP amplitude had at least partially recovered indicating viability of the preparation. Lidocaine (12 mM) was applied directly into the recording chamber to identify the electrical stimulus artifact. The concentration of A803467 used was ~35× the IC_{50} reported to block TTX-r current in rat DRG neurons (Jarvis et al., 2007). In a separate series of experiments performed in Mannheim, nerve segments from WT and $Na_V1.8^{-/-}$ mice were examined. In the control period, nerve segments were maintained at 23 ± 2°C until the latency and amplitude of the C-fiber volley were stable. The tissue was then warmed to 32 ± 2°C and held at this temperature for >5 min or until the recording was stable again. TTX (500 nM) was subsequently added to the perfusing solution for 5 min, after which the temperature was cooled to 23 ± 2°C for an additional 5 min and then rewarmed to 32 ± 2°C. TTX was washed out for ~30 min until C-CAP amplitude reached a plateau and no further increase in the amplitude was observed. In all experiments, except those involving $Na_V1.8^{-/-}$ mice, lidocaine (1 mM) was added to the perfusing solution at the end of the protocol for 5 min at 32 ± 2°C to confirm that the recorded compound action potential signal was mediated by Na_V channels. The TTX concentrations (1 μM and 500 nM) used in these studies are 100–1000× above the IC_{50} required to block TTX-s Na_V channel isoforms and 40,000–60,000 × below the IC_{50} (40–60 mM) reported to block TTX-r isoforms $Na_V1.8$ and $Na_V1.9$ (Catterall et al., 2005), but only a factor of 4 lower than the IC_{50} for $Na_V1.5$ (Renganathan et al., 2002).

Data analysis. For the studies at JHU, from the end of each incubation period (baseline and superfusion with TTX and TTX + A803467), 10 traces of C-CAP recordings were averaged in DAPSYS and data from this average were copied into Excel (Microsoft Office 2010) to determine the peak-to-peak amplitude of the averaged C-CAP waveform (see inset in Fig. 1*D*). For the studies at Mannheim, the peak-to-peak amplitude (see inset in Fig. 1*D*) and latency were determined for CAP responses to each electrical stimulus during the recording by QTRAC software. *Post hoc* data analysis was performed using custom routines written in IgorPro (Wavemetrics). CAP latency and peak-to-peak amplitude were determined by averaging values across three to five sequential sweeps at time points corresponding to the end of the control period, during incubation with TTX, after washing, and during lidocaine. Area under the curve (AUC) of the C-fiber CAP was determined offline by integrating the CAP record over a fixed 25 ms time window beginning 2–3 ms before the C-fiber peak, as determined by inspection.

Statistics. Statistical analyses were performed with Statistica software using nonparametric or parametric tests where appropriate, as described in detail in the Results section. For group comparisons, data are presented as mean ± SEM. p-values < 0.05 were regarded as significant.

Chemicals. Stock solution aliquots of TTX (Tocris Bioscience and Sigma-Aldrich) were prepared in PBS and stored at −20°C. Lidocaine hydrochloride (Samuel Perkins or Sigma-Aldrich) was stored as a stock solution in distilled water at room temperature. Stock solutions were diluted to the desired concentration in physiological solution on the day of the experiment. A803467 (Tocris Bioscience) was initially dissolved in DMSO and serially diluted into physiological solution.

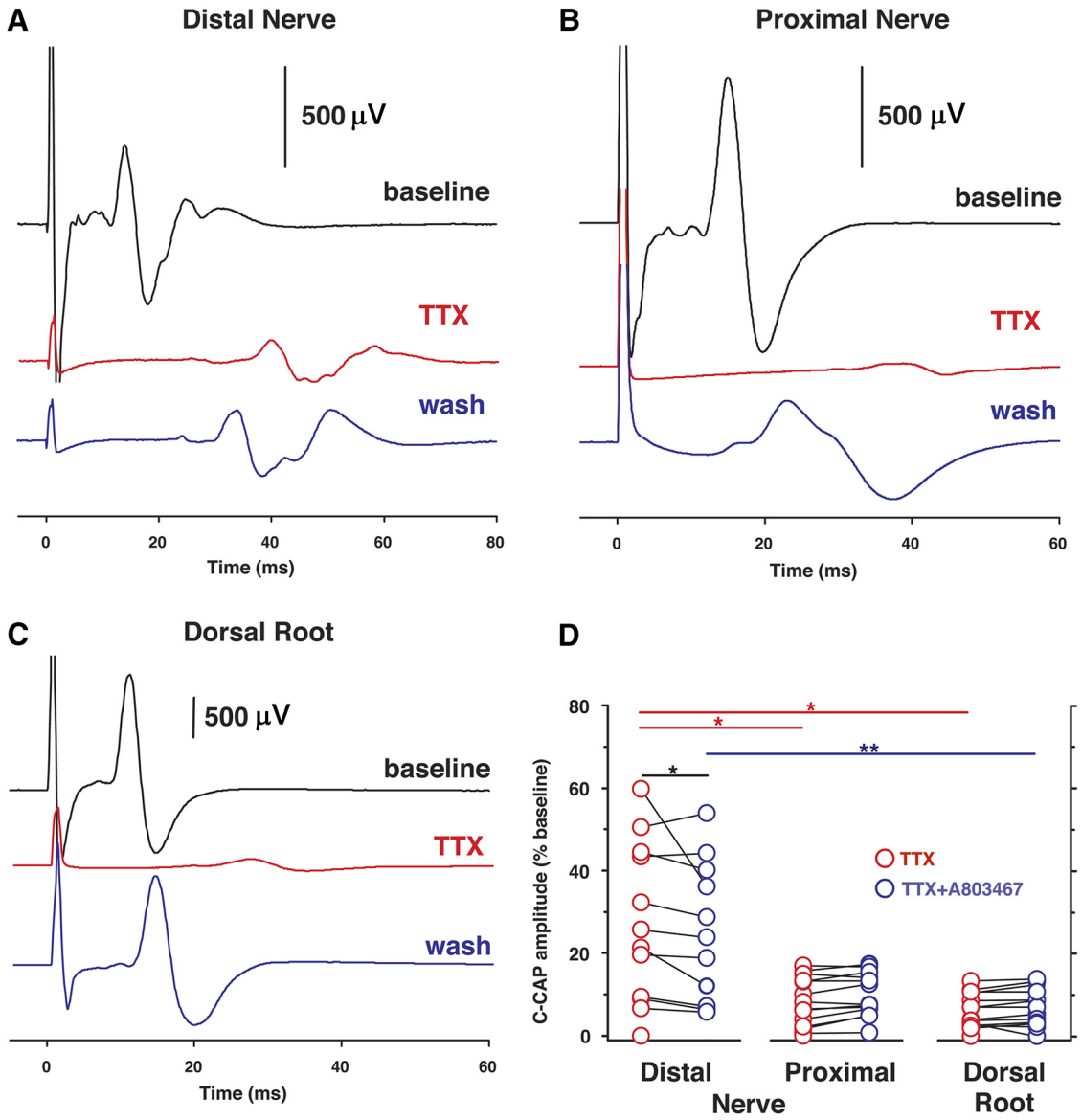

Figure 2. Increased TTX-resistant conduction in distal peripheral nerves of WT mice. ***A–C***. Specimen recordings from distal and proximal nerve and dorsal root, respectively. During superfusion with TTX (1 μM), latency of C-CAP increases and amplitude of C-CAP decreases. Washout leads to recovery of the C-CAP and lidocaine suppresses all neuronal conduction. ***D***, Group data for both TTX (red circles) and TTX plus A803467 (5 μM, blue circles) differed significantly between neuronal compartments ($p = 0.0169$ and $p = 0.008$, respectively, Kruskal–Wallis ANOVA, followed by *post hoc* multiple comparisons). TTX and TTX plus A803467 data obtained from the same nerve sample are connected by lines. For incubation with TTX plus A803467, data were not displayed if TTX alone already completely inhibited C-CAP. On average, 24.7%, 7.1%, and 5.8% of the C-CAP remained under TTX in distal nerves ($n = 13$), proximal nerves ($n = 16$), and dorsal roots ($n = 15$), respectively. Incubation with TTX and A803467 further decreased the amplitude of the remaining C-CAP in distal nerve segments only ($p < 0.05$, Wilcoxon matched pairs, $n = 11$). Significant differences between C-CAP amplitudes of different nerve segments are indicated by red lines (TTX) and blue lines (TTX plus A803467) as detected by *post hoc* multiple comparisons. Black line indicates significantly smaller C-CAP under TTX plus A803467 compared with TTX alone in distal nerve segment. *$p < 0.05$.

Results

One-fourth of the C-CAP signal in distal axonal segments is TTX resistant

We used CAP recordings in combination with pharmacological agents to examine functionally whether there are spatial differences in the contribution of Na_V channel isoforms to conduction along peripheral axons. In particular, we investigated the effects of TTX (1 μM) and a combination of TTX (1 μM) and A803467 (5 μM), a $Na_V1.8$-specific blocker (Jarvis et al., 2007), on conduction in unmyelinated C-fibers in dorsal roots and proximal and distal (digital) segments of peripheral nerve. The C-CAP response to supramaximal electrical stimuli was monitored during superfusion with the different compounds and examples of recordings from different nerve segments from WT mice are shown in Figure 2. In all preparations, TTX (1 μM) slowed C-fiber conduction as evidenced by an increase in response latency of the C-CAP. In distal nerve segments (Fig. 2*A*), a considerable fraction of the control C-CAP amplitude was still apparent at the end of the TTX superfusion period. In contrast, TTX largely suppressed the C-CAP amplitude in proximal nerve segments and dorsal roots (Fig. 2*B*, *C*). During washout, C-CAP recovered partially and subsequent application of lidocaine completely blocked axonal conduction. As can be seen from the example traces, C-CAP amplitude varied considerably between recordings. To quantify effects across different experiments, C-CAP amplitudes were normalized to baseline C-CAP amplitude. For the recordings in Figure 2, *A–C*, the

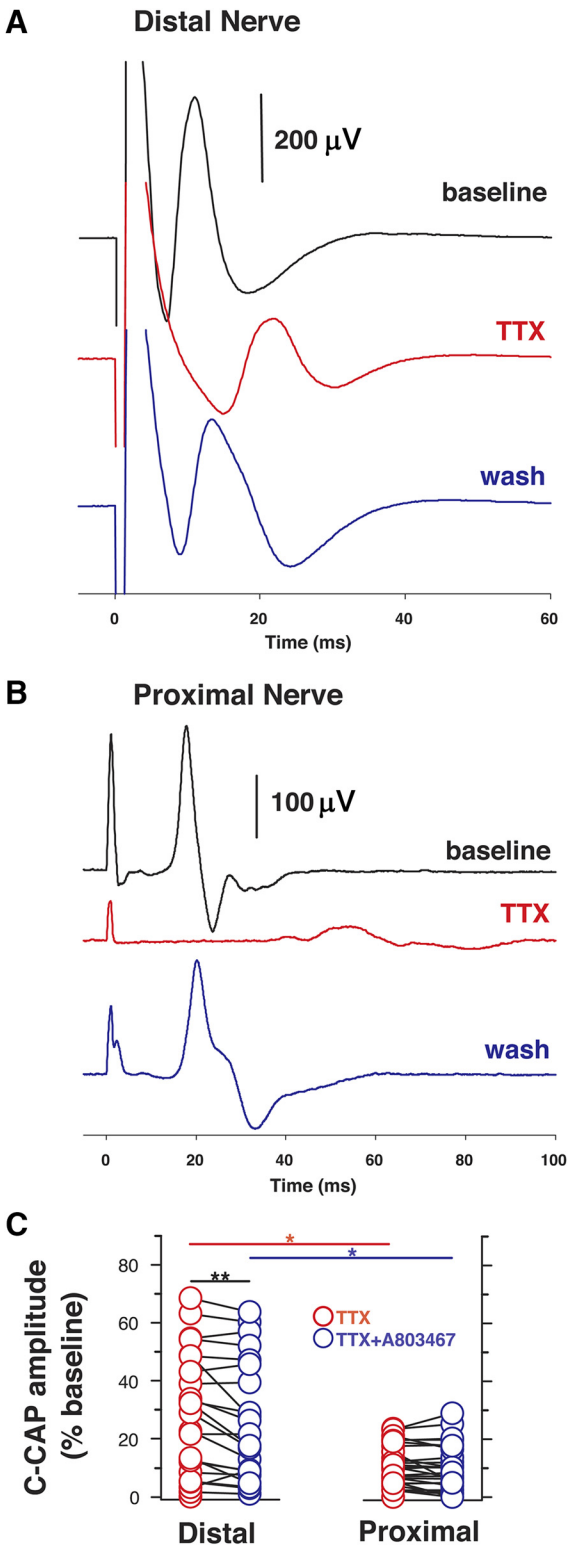

Figure 3. A considerable portion of C-CAP in distal peripheral nerves of macaques is resistant to TTX. ***A***, ***B***, Specimen recording of C-CAPs in distal and proximal nerve, respectively. Superfusion with TTX (1 μM) increases C-CAP latency and decreases C-CAP amplitude. For the specimen from the distal nerve ~33% of C-CAP remained under TTX, whereas ~10% remained in the specimen recording from the proximal nerve. ***C***, Group data for C-CAP from proximal and distal nerves. Normalized C-CAP amplitude under TTX was significantly larger in distal nerves ($n = 27$) than in proximal nerves ($n = 31$, $p = 0.03$, Mann–Whitney *U* test). Similarly, the C-CAP amplitude during incubation with TTX (1 μM) and A803467 (5 μM) was larger in distal nerves ($n = 22$) than in proximal segments ($n = 26$, $p = 0.01$, Mann–Whitney *U* test). Only in distal nerve segments did the C-CAP amplitude significantly decrease under incubation with TTX and A803467 compared with TTX alone ($n = 22$, $p = 0.0041$, Wilcoxon matched pairs). Red (blue) lines indicate significant differences for TTX (TTX plus A803467) between distal and proximal nerve segments. Black line indicates significant difference in C-CAP amplitude between TTX and TTX plus A803467 in distal nerve segments. *$p < 0.05$; **$p < 0.01$.

normalized C-CAP in the presence of TTX was 25.7% for distal nerve, but only 4.0% and 6.5% for the proximal nerve and dorsal root, respectively. The effect of TTX on C-CAP amplitude differed significantly between neuronal compartments (Fig. 2*D*, Kruskal–Wallis ANOVA, $H_{(2,44)} = 8.16$, $p = 0.017$). During exposure to TTX, C-CAP amplitude was significantly larger in distal nerves (24.7 ± 5.5%, $n = 13$) than in both dorsal roots (5.8 ± 1.2%, $n = 15$) and proximal nerve segments (7.1 ± 1.6%, $n = 16$, $p < 0.05$, *post hoc* multiple comparisons). In distal nerve preparations, but not in dorsal root or proximal nerve preparations, the amplitude of the remaining C-CAP in the presence of TTX varied substantially. In some distal nerves, but not in others, the C-CAP was completely abolished by TTX. Similar to TTX alone, the effect of TTX combined with A803467 differed significantly between different nerve segments (Kruskal–Wallis ANOVA, $H_{(2,37)} = 9.60$, $p = 0.008$), with the TTX-r C-CAP amplitude being significantly larger in distal nerves than dorsal roots ($p = 0.006$, *post hoc* multiple comparisons). Only within the distal nerve segment did the incubation with combined TTX and A803467 further decrease the C-CAP amplitude (25.2 ± 5.1%) compared with TTX alone (29.3 ± 5.5%, $p < 0.05$, Wilcoxon matched pairs, $n = 11$), but this effect was rather small.

To test whether the effects of TTX or combined TTX and A803467 also differed between neuronal compartments in primates, recordings were made from dorsal roots, proximal and distal (digital) nerves from pigtail monkeys. Similar to recordings from WT mice, TTX slowed the C-CAP in all nerve segments. In the distal nerve segments (Fig. 3*A*), the C-CAP was reduced to 21.5% of its control amplitude by TTX (1 μM). In proximal nerve segments (Fig. 3*B*), TTX reduced the C-CAP amplitude to 10% (i.e., by 90%). As in WT mice, primate dorsal roots and proximal nerves did not differ in their response to TTX and data from these tissues were therefore combined for group comparisons (Fig. 3*C*). After incubation with TTX or combined TTX and A803467, the C-CAP amplitude resistant to blockade was significantly larger in distal than proximal nerves (TTX: 24.2 ± 4.2%, $n = 27$, vs 9.4 ± 1.3%, $n = 31$, $p = 0.03$, Mann–Whitney *U* test; TTX/A803467: 25.6 ± 4.4%, $n = 22$, vs 10.2 ± 1.5%, $n = 26$, $p = 0.01$, Mann–Whitney *U* test). In distal, but not proximal, nerve segments, exposure to combined TTX and A803467 reduced C-CAP amplitude compared with TTX alone (TTX vs TTX/A803467: 29.7 ± 4.2% vs 25.6 ± 4.4%, $n = 22$, $p = 0.0041$, Wilcoxon matched pairs), but the effect was again small. Together, the data from mice and nonhuman primates indicate that conduction in a considerable fraction of unmyelinated C-fibers in distal nerves can be mediated by TTX-r Na_V channel isoforms.

Axonal TTX-r C-CAP is present in $Na_V1.9^{-/-}$ mice

In adult mammals, somatosensory C-fiber neurons express the TTX-resistant Na_V channel isoforms $Na_V1.8$ and $Na_V1.9$. To determine the contribution of $Na_V1.9$ to TTX-resistant axonal conduction in C-fibers, C-CAPs were recorded from distal and proximal nerve segments of $Na_V1.9^{-/-}$ mice (Fig. 4*A*,*B*). The effect of 1 μM TTX on axonal C-fiber conduction in $Na_V1.9^{-/-}$ mice was indistinguishable from its effect on peripheral nerves from WT mice and nonhuman primates. In proximal nerve seg-

←

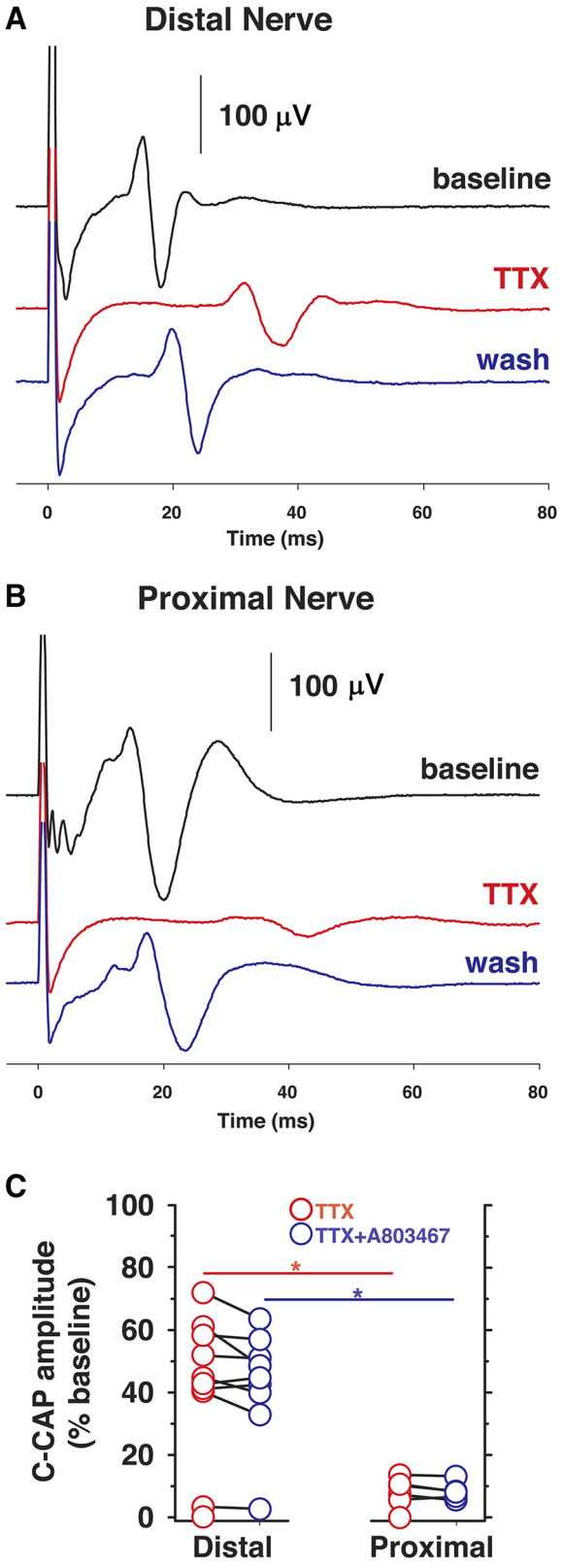

Figure 4. Compared with proximal nerves, a significantly larger portion of C-CAP in distal nerves is TTX resistant in $Na_V1.9^{-/-}$ animals. ***A***, ***B***, Specimen recordings from distal and proximal nerves of $Na_V1.9^{-/-}$ mice, respectively. ***C***, Group data. Significant differences between distal and proximal nerve segments are indicated by red (TTX, 1 μM) and blue lines (TTX plus A803467, 5 μM). For both TTX and TTX plus A803467, amplitudes of remaining C-CAPs were significantly larger in distal than proximal nerve segments ($p < 0.05$, Mann–Whitney *U* test; see text for details). *$p < 0.05$.

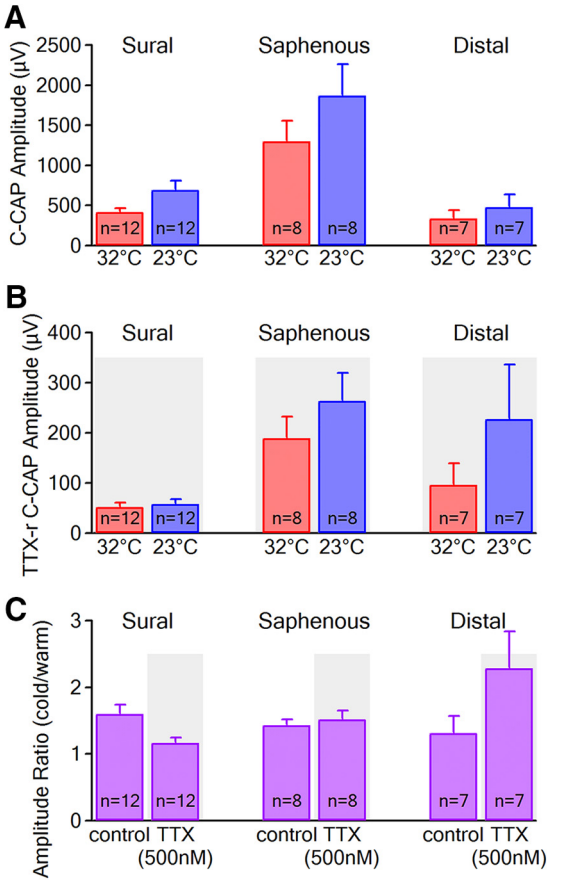

Figure 5. Effect of temperature and TTX (500 nM) on axonal conduction in peripheral C-fibers of WT mice. ***A***, ***B***, Comparison of the absolute C-CAP amplitude in WT mice at 32°C (red bars) and 23°C (blue bars) for proximal sural (left), proximal saphenous (center), and distal (right) nerve segments before (***A***) and during TTX (500 nM; ***B***). ***C***, Amplitude ratio indicating the relative increase in amplitude upon cooling from 32°C to 23°C before (control) and in the presence of TTX (500 nM; gray shading) in proximal sural (left), proximal saphenous (center), and distal (right) nerve segments.

ments, C-CAP was largely blocked by TTX (Fig. 4*B*), whereas 40% of the C-CAP in distal nerve segments was TTX resistant (Fig. 4*A*). Analysis of the group data (Fig. 4*C*) revealed that the amplitudes of the remaining C-CAP during both TTX and combined TTX and A803467 were significantly larger in distal compared with proximal nerve segments (TTX: 41.5 ± 7.4%, $n = 10$, vs 6.8 ± 2.0%, $n = 7$, $p = 0.022$, Mann–Whitney *U* test; TTX plus A803467: 42.5 ± 5.8%, $n = 9$, vs 8.4 ± 1.3%, $n = 5$, $p = 0.022$, Mann–Whitney *U* test). In proximal and distal nerve segments, incubation with TTX and A803467 did not further decrease the C-CAP amplitude (proximal: 9.5 ± 1.4% vs 8.4 ± 1.3, $n = 5$, $p = 0.14$, Wilcoxon matched pairs; distal: 46.1 ± 6.4% vs 42.5 ± 5.8%, ($n = 10$, $p = 0.086$, Wilcoxon matched pairs).

C-CAP amplitude is increased by cooling, primarily in distal axonal segments

In all nerve segments (proximal sural and saphenous as well as distal nerve segments), 500 nM TTX blocked axonal conduction in A-fibers. The A-CAP amplitude was reduced by TTX to 4 ± 2% of its control value (data not shown; 1-way ANOVA, $F_{(1,30)} = 16.81$, $p < 0.01$). Changes in temperature and application of 500 nM TTX were used to characterize TTX-r axonal conduction in peripheral C-fibers. In WT mice, cooling from 32°C to 23°C increased the C-CAP amplitude both before (Fig. 5*A*, control,

repeated-measures ANOVA, with "cooling" as within-subject factor, $F_{(1,24)} = 28$, $p < 0.01$) and during application of TTX (500 nM; Fig. 5*B*, repeated-measures ANOVA, $F_{(1,24)} = 12.87$, $p < 0.01$). There was no difference in the relative increase in amplitude upon cooling before and during TTX treatment (Fig. 5*C*; 2-way ANOVA with "treatment" and "nerve segment" as independent variables; treatment $F_{(1,48)} = 1.27$, $p = 0.26$; nerve segment $F_{(2,48)} = 1.83$, $p = 0.17$). In contrast to cooling, TTX (500 nM) significantly reduced the C-CAP amplitude in all nerves (Fig. 5*A*,*B*) both at 32°C (2-way ANOVA with "treatment" and "nerve segment" as independent variables; treatment $F_{(1,48)} = 42.86$, $p < 0.01$) and 23°C (2-way ANOVA $F_{(1,48)} = 35.3$, $p < 0.01$). Markedly, for nerves from WT mice, there were prominent differences in the absolute C-CAP amplitude across different nerve segments (Fig. 5*A*). Accordingly, to make comparisons between nerves for the effects of TTX and temperature, C-CAP amplitudes were normalized to their control values at 32°C (Fig. 6*A*–*C*). The normalized amplitude of the TTX-r C-CAP for proximal sural (Fig. 6*A*) and saphenous (Fig. 6*B*) nerves was 14% at 32°C and 10–16% at 23°C. In distal nerve segments, 27% of the C-CAP amplitude was TTX-r at 32°C and 57% was TTX-r at 23°C (Fig. 6*C*). Kruskal–Wallis ANOVA indicated a statistically significant difference in TTX-r amplitude between different nerve segments at 23°C (Fig. 6*D*; $H_{(2,27)} = 8.96$, $p < 0.05$), a feature that was not apparent at 32°C (Fig. 6*D*; $H_{(2,27)} = 4.76$, $p = 0.09$). A nonparametric test was used in this analysis because the data violated the assumption of equal variances. To confirm that electrically evoked TTX-r CAPs were mediated by Na_V channels, the broad-spectrum Na_V blocker lidocaine (1 mM) was applied at the end of each experiment (Fig. 6*A*–*C*). Lidocaine blocked C-fiber conduction in all nerve segments, with the amplitude of the C-CAP reduced to 1–3% of its control value (2-way ANOVA with "treatment" and "nerve segment" as independent variables; treatment $F_{(1,46)} = 54.75$, $p < 0.01$). The conduction velocity of the C-CAP under control conditions did not differ in sural, saphenous, or distal nerve segments from WT mice (data not shown; 1-way ANOVA $F_{(2,19)} = 2.97$, $p = 0.08$).

Axonal TTX-r C-fiber conduction is absent in $Na_V1.8^{-/-}$ mice

Transgenic mice lacking $Na_V1.8$ were used to determine the contribution of $Na_V1.8$ to TTX-r CAPs recorded in peripheral nerve segments. In addition, because $Na_V1.8$ resists inactivation during cooling (Zimmermann et al., 2007), the involvement of $Na_V1.8$ in the cooling induced increase in C-CAP amplitude (Fig. 5) was also assessed.

In sural, saphenous, and distal nerve segments from $Na_V1.8^{-/-}$ mice, 500 nM TTX blocked the electrically evoked C-CAP at 32°C (2-way ANOVA with "treatment" and "nerve segment" as independent variables; treatment $F_{(1,54)} = 62.91$, $p < 0.01$) and this effect could not be rescued by cooling to 23°C (Fig. 7*A*–*C*; 2-way ANOVA with "treatment" and "nerve segment" as independent variables; treatment $F_{(1,54)} = 60.45$, $p < 0.01$); that is, there was no detectable axonal TTX-r C-CAP. This observation suggests that $Na_V1.8$ is solely responsible for the TTX-r CAP signal in peripheral mouse nerve. In contrast, the increase in C-CAP amplitude upon cooling was independent of $Na_V1.8$ (cf. WT control in Fig. 6*A*–*C* with $Na_V1.8^{-/-}$ in Fig. 7*A*–*C*). That is, under control conditions, before TTX, the amplitude of C-CAPs from $Na_V1.8^{-/-}$ nerves increased during cooling from 32°C to 23°C (Fig. 7*D*, repeated-measures ANOVA with "cooling" as within-subject factor, $F_{(1,27)} = 14.63$, $p < 0.01$) in a manner comparable to WT nerves (Fig. 5*A*). For all nerves from $Na_V1.8^{-/-}$ mice, blockade of C-fiber conduction by 500 nM TTX was partially reversed by washout. There were no differences in the conduction velocity of the C-CAP under control conditions between different nerve segments from $Na_V1.8^{-/-}$ mice (data not shown; 1-way ANOVA $F_{(2,25)} = 1.68$, $p = 0.21$).

To explore the possibility that block of C-CAPs in nerves from adult $Na_V1.8^{-/-}$ mice might be due to the absence of a subset of C-fiber axons, the absolute amplitude of the C-CAP (Buchthal and Rosenfalck, 1966; Dyck et al., 1971; Tackmann et al., 1976) and the AUC (Stys et al., 1992) of the C-CAP were used as indices of axon number. However, there were no statistically significant differences in either C-CAP amplitude (Fig. 7*E*; 2-way ANOVA; genotype $F_{(1,51)} = 0.76$, $p = 0.39$) or AUC (Fig. 7*F*; 2-way ANOVA; genotype $F_{(1,50)} = 0.44$, $p = 0.51$) between WT and $Na_V1.8^{-/-}$ mice.

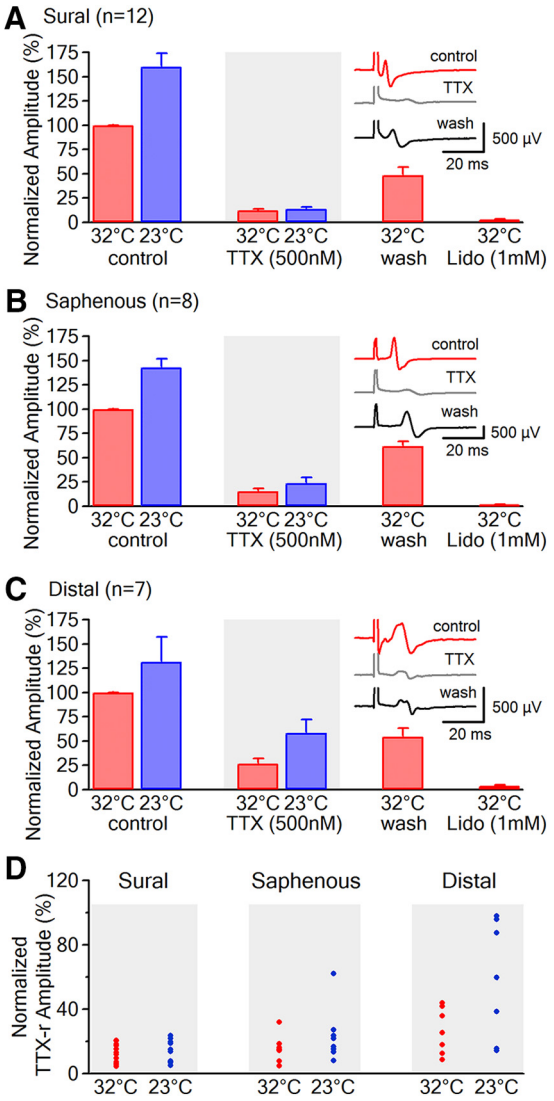

Figure 6. Functional assessment of TTX-r C-fiber conduction in proximal and distal peripheral nerve segments from WT mice. ***A*–*C***, Effect of cooling from 32°C (red bars) to 23°C (blue bars) on the normalized C-CAP amplitude of WT nerves before (control), in the presence of TTX (500 nM, gray shading), after washing, and in the presence of lidocaine (1 mM) for proximal sural (***A***), proximal saphenous (***B***), and distal (***C***) nerve segments of WT mice. Insets in ***A*–*C*** show representative examples of electrically evoked C-CAPs before (top, red trace), during TTX (500 nM; center, gray trace), and after washing (bottom, black trace). ***D***, Individual TTX-r C-CAP amplitudes at 32°C (red circles) and 23°C (blue circles) for proximal sural (left), proximal saphenous (center), and distal (right) nerve segments.

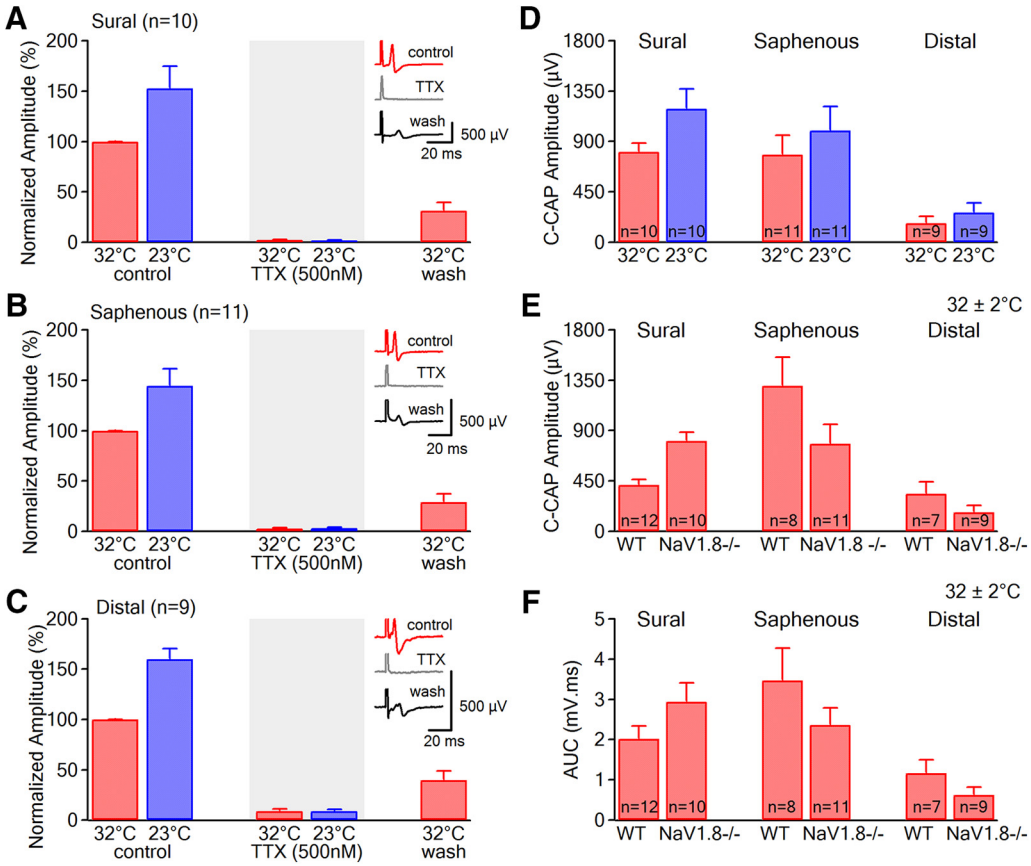

Figure 7. Functional assessment of TTX-r C-fiber conduction in proximal and distal peripheral nerve segments from $Na_V1.8^{-/-}$ mice. ***A–C***, Effect of cooling from 32°C (red bars) to 23°C (blue bars) on the normalized C-CAP amplitude of $Na_V1.8^{-/-}$ nerves before (control), in the presence of TTX (500 nM, gray shading) and after washing for proximal sural (***A***), proximal saphenous (***B***), and distal (***C***) nerve segments. ***D***, C-CAP amplitude in $Na_V1.8^{-/-}$ mice for proximal sural (left), proximal saphenous (center), and distal (right) nerve segments at 32°C (red bars) and 23°C (blue bars). ***E***, Comparison of C-CAP amplitude under control conditions between WT and $Na_V1.8^{-/-}$ mice in proximal sural (left), proximal saphenous (center), and distal (right) nerve segments. ***F***, Comparison of the AUC of the C-CAP signal under control conditions between WT and $Na_V1.8^{-/-}$ mice in proximal sural (left), proximal saphenous (center), and distal (right) nerve segments.

Discussion

The results demonstrate that C-CAPs in dorsal roots and proximal nerve segments of mice and nonhuman primates were largely abolished by TTX (0.5–1 μM), whereas in distal nerves, a more considerable portion of the C-fiber signal was resistant to TTX. These findings indicate that C-fiber conduction in proximal nerves and dorsal roots depends largely on TTX-s Na_V channel isoforms, whereas in distal axonal segments, more C-fibers can support TTX-r action potential conduction. Using transgenic mice, $Na_V1.8$ was identified as the sole isoform responsible for axonal TTX-r action potential conduction in C-fibers and the distribution of $Na_V1.8$ was site dependent, with this channel being available functionally at distal axon sites involved in action potential initiation as well as conduction. In contrast, $Na_V1.9$ does not contribute substantially to the ability to generate and conduct a TTX-resistant axonal action potential.

Previous studies have shown that TTX-r Na_V channels are functional in peripheral terminals of unmyelinated afferent nerve fibers (Brock et al., 1998; Brock et al., 2001; Carr et al., 2002; Zimmermann et al., 2007). The present study extends this concept by showing that $Na_V1.8$ underlies TTX-r action potential conduction in C-fiber axons and that TTX-r conduction is enriched in the distal peripheral axonal branches of pseudounipolar DRG C-type neurons. Although immunohistochemical techniques indicate that $Na_V1.8$ and $Na_V1.9$ appear to cluster along the course of unmyelinated axons (Fjell et al., 2000; Rush et al., 2005) and at nerve terminals (Black et al., 2002), no variation in signal intensity along the sciatic nerve has been reported. In neurites of cultured mouse DRG neurons, fluorescently tagged $Na_V1.8$ clustered in lipid rafts along the neuronal membrane but were not enriched in the terminal regions (Pristerà et al., 2012). It is currently unclear how the observed spatial differences in our functional assay of $Na_V1.8$ might occur. The preferential availability of $Na_V1.8$ in distal axon segments and terminals may involve mechanisms related to local protein translation (Jiménez-Díaz et al., 2008; Thakor et al., 2009; Obara and Hunt, 2014), channel trafficking, membrane insertion (for reviews, see Swanwick et al., 2010; Bao, 2015), and regulation of channel function, for example, through phosphorylation and Na_V channel β-subunits (for review, see Ahern et al., 2016). Our observation that TTX-r channels support conduction in only a limited number of unmyelinated axons in proximal nerves or dorsal roots is consistent with previous functional observations in rats indicating that TTX-r Na_V channel isoforms alone were not sufficient for synaptic transmission of nociceptive input within the dorsal horn (Pinto et al., 2008). Together, previous and present findings suggest that TTX-r Na_V channel isoforms are functionally relevant in peripheral terminals and distal axons of unmyelinated fibers.

Several factors could contribute to the observation of a larger TTX-r CAP in distal nerve segments. For example, more prominent diffusion barriers could limit access of TTX to unmyelinated fibers in distal nerve segments. Although all nerves were desheathed

to remove the perineurium/epineurium, which is known to impair access of TTX to peripheral axons (Hackel et al., 2012), we consider hampered toxin diffusion unlikely because TTX fully blocked A-fibers in all preparations and similarly abolished C-CAPs in distal nerves from $Na_V1.8^{-/-}$ animals (Fig. 7*C*), demonstrating that TTX had access to unmyelinated axons.

We did not observe a biologically significant effect of A803467 on TTX-r CAPs in distal nerves. Currently, we cannot explain this limited effect because A803467 has been shown previously to block transient and resurgent TTX-r current in isolated rat DRG neurons (Jarvis et al., 2007; Tan et al., 2014). However, the state-dependent affinity for inactivated $Na_V1.8$ led to effects of A803467 on TTX-r current in DRG neurons that were dependent on membrane potential (Jarvis et al., 2007), a parameter not controlled in our axonal recordings. Furthermore, the efficacy of A803467 on C-CAPs may be larger after peripheral nerve injury or inflammation. In models of chronic pain, but not in naive rats, A803467 effectively reduced nociceptive behavior and inhibited spontaneous and evoked activity in wide dynamic range dorsal horn neurons (Jarvis et al., 2007; McGaraughty et al., 2008; Joshi et al., 2009; Liu et al., 2014; Rahman and Dickenson, 2015).

Our results with $Na_V1.8^{-/-}$ nerves support the notion that TTX-r-resistant C-CAPs are mediated by $Na_V1.8$. Like its effect in WT animals, TTX only partially reduced C-CAPs in peripheral nerves from $Na_V1.9^{-/-}$ animals, suggesting that $Na_V1.9$ contributes minimally to TTX-r C-CAPs. Interestingly, the TTX-resistant C-CAP in sural and saphenous nerves from $Na_V1.9^{-/-}$ mice appeared to be larger than in WT (~20% vs 40%; cf. Figs. 3*C*, 4*C*), a result that may indicate compensatory overexpression of $Na_V1.8$ in distal nerves of such animals.

During cooling, axonal action potentials slow in conduction speed and increase in amplitude (Hodgkin and Katz, 1949; Swadlow et al., 1981; Stys et al., 1992; Sittl et al., 2012; Fig. 5). The reduction in conduction speed is attributed to a slowing of the activation time constant of Na_V channels (Frankenhaeuser and Moore, 1963). The increase in CAP amplitude with cooling is also attributed primarily to changes in Na_V kinetics. Cooling slows the rate of both Na_V activation and inactivation with the Q_{10} for inactivation ($Q_{10} = 2.8$) exceeding that for activation (Frankenhaeuser and Moore, 1963; Kimura and Meves, 1979; Collins and Rojas, 1982; Schwarz and Eikhof, 1987) ($Q_{10} = 1.8$), prolonging Na_V channel opening time and thus action potential amplitude. In addition, membrane resistance increases substantially during cooling (Reid and Flonta, 2002) primarily due to the temperature-dependent closure of two-pore-domain potassium channels (Maingret et al., 2000; Kang et al., 2005; Schneider et al., 2014). The resulting increase in resistance amplifies the effect of Na_V-channel mediated current on voltage.

Here, we confirm that cooling increased the amplitude and AUC of C-CAPs in nerves from WT and $Na_V1.8^{-/-}$ mice (Figs. 6, 7). Therefore, a component of temperature-dependent changes in CAP shape occurs independently of $Na_V1.8$. The pronounced effect of cooling on distal nerve segments of WT tissue might therefore suggest an enrichment of both $Na_V1.8$ and perhaps background potassium currents in the most distal axonal compartment.

A possible explanation for the observation that conduction in all C-fiber axons is sensitive to TTX in $Na_V1.8^{-/-}$ mice is that select populations of DRG neurons are impaired developmentally, thereby leading to axonal loss. Specifically, a reduction in the number of IB4-positive and CGRP-positive DRG neurons might be expected based upon diphtheria ablation in $Na_V1.8$-expressing neurons (Abrahamsen et al., 2008). However, an analysis of C-CAP amplitude and AUC as indices of axon number suggests that the number of C-fiber axons did not differ significantly between WT and $Na_V1.8^{-/-}$ mice (Fig. 7*E*,*F*). Similarly, in the original description of this $Na_V1.8$-null transgenic line, DRG neuronal counts and immounohistochemical ratios were both taken to indicate no neuronal loss after global deletion of the channel (Akopian et al., 1999). Although our indices of axon number (C-CAP amplitude and AUC) indicated no loss of axons in $Na_V1.8^{-/-}$ nerves, it should be noted that these indices varied depending upon the nerve tested (Fig. 7*E*,*F*). Compared with WT, $Na_V1.8^{-/-}$ mice showed larger C-CAP amplitude and AUC for sural nerve segments, but lower values for saphenous and distal nerve segments. This apparent inconsistency across nerves may suggest that loss of $Na_V1.8$ results in different compensatory mechanisms in different nerves and is perhaps dependent on the proportion of sensory and sympathetic fibers or the ratio of C- to A-fibers. Immunohistochemical studies using $Na_V1.8$-specific antibodies (Amaya et al., 2000) and studies using a $Na_V1.8$-Cre mouse line (Abrahamsen et al., 2008; Shields et al., 2012) showed colocalization of $Na_V1.8$ and the A-fiber-associated heavy-chain neurofilament marker NF200. Similarly, single-cell analysis revealed $Na_V1.8$ expression in large-diameter DRG neurons overlapping with NF200 expression (Ho and O'Leary, 2011).

We observed that $Na_V1.8$ was functional in distal peripheral nerves of mice (Fig. 2), consistent with the proposal that this channel likely plays an important role in distal axons of unmyelinated afferents. Behaviorally, $Na_V1.8$-deficient mice display a delayed onset of inflammatory hyperalgesia after complete Freund's adjuvant (CFA) and reduced sensitivity to painful mechanical and cold stimuli (Akopian et al., 1999; Zimmermann et al., 2007). Antisense oligodeoxynucleotide targeting $Na_V1.8$, but not $Na_V1.9$, increased paw withdrawal thresholds in rats after intraplantar CFA (Yu et al., 2011). Spinal nerve injury induced an upregulation of $Na_V1.8$ in uninjured fibers of the sciatic nerve (Gold et al., 2003) and knockdown of $Na_V1.8$ reversed signs of neuropathic pain in animal models (Lai et al., 2002; Yang et al., 2014) and reduced spontaneous activity in dissociated DRG neurons after spinal cord injury (Yang et al., 2014). In humans, $Na_V1.8$-gain-of-function mutations have been observed in patients with painful distal neuropathy (Faber et al., 2012) and $Na_V1.8$ was significantly increased in painful lingual nerve injury neuromas (Bird et al., 2013). Collectively, these studies suggest that $Na_V1.8$ plays a crucial role in peripheral nociceptive signaling. The results from our studies indicate that $Na_V1.8$ is not only functional in peripheral, receptive terminals, but also in distal axons of mice and nonhuman primates. Accordingly, therapeutic targeting of $Na_V1.8$ in peripheral tissues (e.g., at sites of injury) may provide a strategy for the relief of pain of peripheral origin while avoiding central side effects.

References

Abrahamsen B, Zhao J, Asante CO, Cendan CM, Marsh S, Martinez-Barbera JP, Nassar MA, Dickenson AH, Wood JN (2008) The cell and molecular basis of mechanical, cold, and inflammatory pain. Science 321:702–705. CrossRef Medline

Ahern CA, Payandeh J, Bosmans F, Chanda B (2016) The hitchhiker's guide to the voltage-gated sodium channel galaxy. J Gen Physiol 147:1–24. CrossRef Medline

Akopian AN, Souslova V, England S, Okuse K, Ogata N, Ure J, Smith A, Kerr BJ, McMahon SB, Boyce S, Hill R, Stanfa LC, Dickenson AH, Wood JN (1999) The tetrodotoxin-resistant sodium channel SNS has a specialized function in pain pathways. Nat Neurosci 2:541–548. CrossRef Medline

Amaya F, Decosterd I, Samad TA, Plumpton C, Tate S, Mannion RJ, Costigan M, Woolf CJ (2000) Diversity of expression of the sensory neuron-

specific TTX-resistant voltage-gated sodium ion channels SNS and SNS2. Mol Cell Neurosci 15:331–342. CrossRef Medline

Bao L (2015) Trafficking regulates the subcellular distribution of voltage-gated sodium channels in primary sensory neurons. Mol Pain 11:61. CrossRef Medline

Bird EV, Christmas CR, Loescher AR, Smith KG, Robinson PP, Black JA, Waxman SG, Boissonade FM (2013) Correlation of Nav1.8 and Nav1.9 sodium channel expression with neuropathic pain in human subjects with lingual nerve neuromas. Mol Pain 9:52. CrossRef Medline

Black JA, Renganathan M, Waxman SG (2002) Sodium channel Nav1.6 is expressed along nonmyelinated axons and it contributes to conduction. Brain Res Mol Brain Res 105:19–28. CrossRef Medline

Blair NT, Bean BP (2002) Roles of tetrodotoxin (TTX)-sensitive Na+ current, TTX-resistant Na+ current, and Ca2+ current in the action potentials of nociceptive sensory neurons. J Neurosci 22:10277–10290. Medline

Brock JA, McLachlan EM, Belmonte C (1998) Tetrodotoxin-resistant impulses in single nociceptor nerve terminals in guinea-pig cornea. J Physiol 512:211–217. CrossRef Medline

Brock JA, Pianova S, Belmonte C (2001) Differences between nerve terminal impulses of polymodal nociceptors and cold sensory receptors of the guinea-pig cornea. J Physiol 533:493–501. CrossRef Medline

Buchthal F, Rosenfalck P (1966) Spontaneous electrical activity of human muscle. Electroencephalogr Clin Neurophysiol 20:321–336. CrossRef Medline

Carr RW, Pianova S, Brock JA (2002) The effects of polarizing current on nerve terminal impulses recorded from polymodal and cold receptors in the guinea-pig cornea. J Gen Physiol 120:395–405. CrossRef Medline

Carr RW, Sittl R, Fleckenstein J, Grafe P (2010) GABA increases electrical excitability in a subset of human unmyelinated peripheral axons. PLoS One 5:e8780. CrossRef Medline

Catterall WA, Goldin AL, Waxman SG (2005) International Union of Pharmacology. XLVII. Nomenclature and structure-function relationships of voltage-gated sodium channels. Pharmacol Rev 57:397–409. CrossRef Medline

Collins CA, Rojas E (1982) Temperature dependence of the sodium channel gating kinetics in the node of Ranvier. Q J Exp Physiol 67:41–55. CrossRef Medline

De Col R, Messlinger K, Carr RW (2008) Conduction velocity is regulated by sodium channel inactivation in unmyelinated axons innervating the rat cranial meninges. J Physiol 586:1089–1103. CrossRef Medline

Dyck PJ, Lambert EH, Sanders K, O'Brien PC (1971) Severe hypomyelination and marked abnormality of conduction in Dejerine-Sottas hypertrophic neuropathy: myelin thickness and compound action potential of sural nerve in vitro. Mayo Clin Proc 46:432–436. Medline

Faber CG, Lauria G, Merkies IS, Cheng X, Han C, Ahn HS, Persson AK, Hoeijmakers JG, Gerrits MM, Pierro T, Lombardi R, Kapetis D, Dib-Hajj SD, Waxman SG (2012) Gain-of-function Nav1.8 mutations in painful neuropathy. Proc Natl Acad Sci U S A 109:19444–19449. CrossRef Medline

Farrag KJ, Costa SK, Docherty RJ (2002) Differential sensitivity to tetrodotoxin and lack of effect of prostaglandin E2 on the pharmacology and physiology of propagated action potentials. Br J Pharmacol 135:1449–1456. CrossRef Medline

Fjell J, Hjelmström P, Hormuzdiar W, Milenkovic M, Aglieco F, Tyrrell L, Dib-Hajj S, Waxman SG, Black JA (2000) Localization of the tetrodotoxin-resistant sodium channel NaN in nociceptors. Neuroreport 11:199–202. CrossRef Medline

Frankenhaeuser B, Moore LE (1963) The effect of temperature on the sodium and potassium permeability changes in myelinated nerve fibres of *Xenopus laevis*. J Physiol 169:431–437. CrossRef Medline

Freysoldt A, Fleckenstein J, Lang PM, Irnich D, Grafe P, Carr RW (2009) Low concentrations of amitriptyline inhibit nicotinic receptors in unmyelinated axons of human peripheral nerve. Br J Pharmacol 158:797–805. CrossRef Medline

Gold MS, Weinreich D, Kim CS, Wang R, Treanor J, Porreca F, Lai J (2003) Redistribution of $Na_v1.8$ in uninjured axons enables neuropathic pain. J Neurosci 23:158–166. Medline

Hackel D, Krug SM, Sauer RS, Mousa SA, Bocker A, Pflücke D, Wrede EJ, Kistner K, Hoffmann T, Niedermirtl B, Sommer C, Bloch L, Huber O, Blasig IE, Amasheh S, Reeh PW, Fromm M, Brack A, Rittner HL (2012) Transient opening of the perineurial barrier for analgesic drug delivery. Proc Natl Acad Sci U S A 109:E2018–E2027. CrossRef Medline

Ho C, O'Leary ME (2011) Single-cell analysis of sodium channel expression in dorsal root ganglion neurons. Mol Cell Neurosci 46:159–166. CrossRef Medline

Hodgkin AL, Katz B (1949) The effect of temperature on the electrical activity of the giant axon of the squid. J Physiol 109:240–249. CrossRef Medline

Jarvis MF, et al. (2007) A-803467, a potent and selective Nav1.8 sodium channel blocker, attenuates neuropathic and inflammatory pain in the rat. Proc Natl Acad Sci U S A 104:8520–8525. CrossRef Medline

Jeftinija S (1994) The role of tetrodotoxin-resistant sodium channels of small primary afferent fibers. Brain Res 639:125–134. CrossRef Medline

Jiménez-Díaz L, Géranton SM, Passmore GM, Leith JL, Fisher AS, Berliocchi L, Sivasubramaniam AK, Sheasby A, Lumb BM, Hunt SP (2008) Local translation in primary afferent fibers regulates nociception. PLoS One 3:e1961. CrossRef Medline

Joshi SK, Honore P, Hernandez G, Schmidt R, Gomtsyan A, Scanio M, Kort M, Jarvis MF (2009) Additive antinociceptive effects of the selective Nav1.8 blocker A-803467 and selective TRPV1 antagonists in rat inflammatory and neuropathic pain models. J Pain 10:306–315. CrossRef Medline

Kang D, Choe C, Kim D (2005) Thermosensitivity of the two-pore domain K+ channels TREK-2 and TRAAK. J Physiol 564:103–116. CrossRef Medline

Kerr NC, Gao Z, Holmes FE, Hobson SA, Hancox JC, Wynick D, James AF (2007) The sodium channel Nav1.5a is the predominant isoform expressed in adult mouse dorsal root ganglia and exhibits distinct inactivation properties from the full-length Nav1.5 channel. Mol Cell Neurosci 35:283–291. CrossRef Medline

Kimura JE, Meves H (1979) The effect of temperature on the asymmetrical charge movement in squid giant axons. J Physiol 289:479–500. CrossRef Medline

Lai J, Gold MS, Kim CS, Bian D, Ossipov MH, Hunter JC, Porreca F (2002) Inhibition of neuropathic pain by decreased expression of the tetrodotoxin-resistant sodium channel, NaV1.8. Pain 95:143–152. CrossRef Medline

Lang PM, Fleckenstein J, Passmore GM, Brown DA, Grafe P (2008) Retigabine reduces the excitability of unmyelinated peripheral human axons. Neuropharmacology 54:1271–1278. CrossRef Medline

Liu XD, Yang JJ, Fang D, Cai J, Wan Y, Xing GG (2014) Functional upregulation of nav1.8 sodium channels on the membrane of dorsal root Ganglia neurons contributes to the development of cancer-induced bone pain. PLoS One 9:e114623. CrossRef Medline

Maingret F, Lauritzen I, Patel AJ, Heurteaux C, Reyes R, Lesage F, Lazdunski M, Honoré E (2000) TREK-1 is a heat-activated background K+ channel. EMBO J 19:2483–2491. CrossRef Medline

McGaraughty S, Chu KL, Scanio MJ, Kort ME, Faltynek CR, Jarvis MF (2008) A selective Nav1.8 sodium channel blocker, A-803467 [5-(4-chlorophenyl-N-(3,5-dimethoxyphenyl)furan-2-carboxamide], attenuates spinal neuronal activity in neuropathic rats J Pharmacol Exp Ther 324:1204–1211. Medline

Obara I, Hunt SP (2014) Axonal protein synthesis and the regulation of primary afferent function. Dev Neurobiol 74:269–278. CrossRef Medline

Pinto V, Derkach VA, Safronov BV (2008) Role of TTX-sensitive and TTX-resistant sodium channels in Adelta- and C-fiber conduction and synaptic transmission. J Neurophysiol 99:617–628. CrossRef Medline

Priest BT, Murphy BA, Lindia JA, Diaz C, Abbadie C, Ritter AM, Liberator P, Iyer LM, Kash SF, Kohler MG, Kaczorowski GJ, MacIntyre DE, Martin WJ (2005) Contribution of the tetrodotoxin-resistant voltage-gated sodium channel $Na_V1.9$ to sensory transmission and nociceptive behavior. Proc Natl Acad Sci U S A 102:9382–9387. CrossRef Medline

Pristerà A, Baker MD, Okuse K (2012) Association between tetrodotoxin resistant channels and lipid rafts regulates sensory neuron excitability. PLoS One 7:e40079. CrossRef Medline

Quasthoff S, Grosskreutz J, Schröder JM, Schneider U, Grafe P (1995) Calcium potentials and tetrodotoxin-resistant sodium potentials in unmyelinated C fibres of biopsied human sural nerve. Neuroscience 69:955–965. CrossRef Medline

Rahman W, Dickenson AH (2015) Osteoarthritis-dependent changes in antinociceptive action of Nav1.7 and Nav1.8 sodium channel blockers: An in vivo electrophysiological study in the rat. Neuroscience 295:103–116. CrossRef Medline

Reid G, Flonta ML (2002) Ion channels activated by cold and menthol in cultured rat dorsal root ganglion neurones. Neurosci Lett 324:164–168. CrossRef Medline

Renganathan M, Cummins TR, Waxman SG (2001) Contribution of Nav1.8 sodium channels to action potential electrogenesis in DRG neurons. J Neurophysiol 86:629–640. Medline

Renganathan M, Dib-Hajj S, Waxman SG (2002) Nav1.5 underlies the 'third TTX-R sodium current' in rat small DRG neurons. Brain Res Mol Brain Res 106:70–82. CrossRef Medline

Ruangsri S, Lin A, Mulpuri Y, Lee K, Spigelman I, Nishimura I (2011) Relationship of axonal voltage-gated sodium channel 1.8 ($Na_V1.8$) mRNA accumulation to sciatic nerve injury-induced painful neuropathy in rats. J Biol Chem 286:39836–39847. CrossRef Medline

Rush AM, Craner MJ, Kageyama T, Dib-Hajj SD, Waxman SG, Ranscht B (2005) Contactin regulates the current density and axonal expression of tetrodotoxin-resistant but not tetrodotoxin-sensitive sodium channels in DRG neurons. Eur J Neurosci 22:39–49. CrossRef Medline

Schneider ER, Anderson EO, Gracheva EO, Bagriantsev SN (2014) Temperature sensitivity of two-pore (K2P) potassium channels. Curr Top Membr 74:113–133. CrossRef Medline

Scholz A, Kuboyama N, Hempelmann G, Vogel W (1998) Complex blockade of TTX-resistant Na+ currents by lidocaine and bupivacaine reduce firing frequency in DRG neurons. J Neurophysiol 79:1746–1754. Medline

Schwarz JR, Eikhof G (1987) Na currents and action potentials in rat myelinated nerve fibres at 20 and 37deg C. Pflugers Arch 409:569–577. CrossRef Medline

Shields SD, Ahn HS, Yang Y, Han C, Seal RP, Wood JN, Waxman SG, Dib-Hajj SD (2012) Nav1.8 expression is not restricted to nociceptors in mouse peripheral nervous system. Pain 153:2017–2030. CrossRef Medline

Sittl R, Lampert A, Huth T, Schuy ET, Link AS, Fleckenstein J, Alzheimer C, Grafe P, Carr RW (2012) Anticancer drug oxaliplatin induces acute cooling-aggravated neuropathy via sodium channel subtype $Na_V1.6$-resurgent and persistent current. Proc Natl Acad Sci U S A 109:6704–6709. CrossRef Medline

Steffens H, Hoheisel U, Eek B, Mense S (2001) Tetrodotoxin-resistant conductivity and spinal effects of cutaneous C-fibre afferents in the rat. Neurosci Res 39:413–419. CrossRef Medline

Stys PK, Waxman SG, Ransom BR (1992) Effects of temperature on evoked electrical activity and anoxic injury in CNS white matter. J Cereb Blood Flow Metab 12:977–986. CrossRef Medline

Swadlow HA, Waxman SG, Weyand TG (1981) Effects of variations in temperature on impulse conduction along nonmyelinated axons in the mammalian brain. Exp Neurol 71:383–389. CrossRef Medline

Swanwick RS, Pristerà A, Okuse K (2010) The trafficking of $Na_V1.8$. Neurosci Lett 486:78–83. CrossRef Medline

Tackmann W, Spalke G, Oginszus HJ (1976) Quantitative histometric studies and relation of number and diameter of myelinated fibres to electrophysiological parameters in normal sensory nerves of man. J Neurol 212:71–84. CrossRef Medline

Tan ZY, Piekarz AD, Priest BT, Knopp KL, Krajewski JL, McDermott JS, Nisenbaum ES, Cummins TR (2014) Tetrodotoxin-resistant sodium channels in sensory neurons generate slow resurgent currents that are enhanced by inflammatory mediators. J Neurosci 34:7190–7197. CrossRef Medline

Thakor DK, Lin A, Matsuka Y, Meyer EM, Ruangsri S, Nishimura I, Spigelman I (2009) Increased peripheral nerve excitability and local $Na_V1.8$ mRNA up-regulation in painful neuropathy. Mol Pain 5:14. CrossRef Medline

Villière V, McLachlan EM (1996) Electrophysiological properties of neurons in intact rat dorsal root ganglia classified by conduction velocity and action potential duration. J Neurophysiol 76:1924–1941. Medline

Yang Q, Wu Z, Hadden JK, Odem MA, Zuo Y, Crook RJ, Frost JA, Walters ET (2014) Persistent pain after spinal cord injury is maintained by primary afferent activity. J Neurosci 34:10765–10769. CrossRef Medline

Yoshida S, Matsuda Y (1979) Studies on sensory neurons of the mouse with intracellular-recording and horseradish peroxidase-injection techniques. J Neurophysiol 42:1134–1145. Medline

Yu YQ, Zhao F, Guan SM, Chen J (2011) Antisense-mediated knockdown of $Na_V1.8$, but not $Na_V1.9$, generates inhibitory effects on complete Freund's adjuvant-induced inflammatory pain in rat. PLoS One 6:e19865. CrossRef Medline

Zimmermann K, Leffler A, Babes A, Cendan CM, Carr RW, Kobayashi J, Nau C, Wood JN, Reeh PW (2007) Sensory neuron sodium channel Nav1.8 is essential for pain at low temperatures. Nature 447:855–858. Medline